J. Amer. Soc. Hort. Sci. 112(3):545–554. 1987.

Diurnal Changes in Fixation, Transport, and Allocation of Carbon in the Sweet Potato Using ^{11}C Tracer

S.J. Kays
Department of Horticulture, University of Georgia, Athens, GA 30602

J.D. Goeschl, C.E. Magnuson, and Y. Fares
Industrial Engineering and Soil and Crop Sciences, Texas A&M University, College Station, TX 77843

Additional index words. *Ipomoea batatas*, $^{11}CO_2$

Abstract. **Fully expanded apical leaves of *Ipomoea batatas* (L.) Lam. cv. Jewel were exposed three times during the day to a square wave of $^{11}CO_2$ for sufficient duration to approach steady-state isotope equilibrium in the plant. This procedure allowed monitoring of changes in the storage of photosynthate within the treated leaf and the transport and allocation of this carbon throughout the plant during the day. Early in the day, export of photosynthate from the treated leaf predominated over storage (57:43%). By mid-day, export had declined to a point that storage was favored (44:56%). Toward late afternoon, export again increased (54:46%). These changes in the allocation of carbon within the leaf were reflected by alterations in the size and turn-over time of the export pool of photosynthates within the labeled leaf. The latter increased progressively from early morning (19 min) until late afternoon (27 min). The speed of photosynthate transport within the plant varied with position along the main stem. Speeds up to 6 cm·min^{-1} were found between short segments of the stem (i.e. ≈10 cm). As the distance between sites increased, slow and fast rates were averaged, giving mean speeds of 2.0 to 2.5 cm·min^{-1}. The speed of transport also changed during the day and depended, in part, on the position of the transport path along the main stem. Virtually no carbon was translocated acropetally from labeled fully expanded apical leaves during the day. Although some photosynthate was translocated into lateral branches developing at the base of the plant, the predominate sink was the root system.**

Unlike most domesticated plants grown for staple foods, root and tuber crops have evolved survival and reproductive strategies in which accrued carbon is stored in specialized fleshy organs. It is evident from net carbon allocation patterns in these plants at harvest that the interrelationship between the aboveground plant parts and their root system is distinctly different from other domesticates. One of but a number of important differences can be seen in the storage organ per se. The storage root of the sweet potato represents a highly plastic sink in contrast to storage sites in crops such as cereal grains. In the sweet potato, both the volume and length of time for deposition of carbon are not rigidly fixed, while cereals have a relatively short period in which photosynthates are deposited into a fixed potential volume (19).

Although sweet potato is ranked sixth in world production, surprisingly little is known about its carbon acquisition, transport, and allocation system (19). From dry matter partitioning studies between grafted plants with varying propensities for the formation of storage roots, it is evident that storage root sink strength is an important factor affecting final yield (10–12). In addition, leaf age and position can influence the fixation and transport of carbon by the plant (14–18). Thus, both the absolute flux of photosynthate and the directional allocation are important in determining yield.

The carbon fixation, transport, and allocation system of the sweet potato changes not only as the plant develops during the growing season but also during the normal daily light-dark cycle. To understand the operative mechanisms modulating eventual yield, we studied short-term changes in the carbon fixation, transport, and allocation system of the sweet potato.

Received for publication 10 Jan. 1986. The cost of publishing this paper was defrayed in part by the payment of page charges. Under postal regulations, this paper therefore must be hereby marked *advertisement* solely to indicate this fact.

To accomplish this, we used the short-lived isotope ^{11}C, which has a number of distinct advantages over the long-lived isotope ^{14}C. ^{11}C decays by positron-emission, followed by a nuclear annihilation reaction that emits two 0.5-million volt γ-rays at an orientation of 180° to one another (21). The primary advantages of ^{11}C are that it: a) emits a form of radiation that can be measured quantitatively, in real time, and nondestructively in live objects; b) it decays quickly (half-life = 20.4 min) to background levels, allowing experiments to be conducted repeatedly on the same plant; and c) it allows coincidence counting and positron-emission tomographic imaging.

Materials and Methods

The research was conducted at the Duke University Phytotron due to the availability of a 4-MeV Van de Graaff accelerator nearby (≈100 m) in the Physics Dept. Nuclear Laboratory.

Plant material. Sweet potato plants of the cultivar Jewel were grown in 29.5-cm-diameter plastic pots containing 1.33 Terface : 1.33 vermiculite : 1.33 gravel : 1 Norfolk sandy loam (by volume). The plants were held in controlled environmental chambers at the Phytotron under the following conditions: 28° day/24°C night temperatures, 15-hr photoperiod (0700 to 2200 HR) of 600 μmol·s^{-1}m^{-2} combined fluorescent–incandescent light, and an ambient CO_2 concentration of 350 cm^3·m^{-3}. Due to the filtering out of ultraviolet (UV) radiation by glass heat shields in the top of the growth chambers, we exposed the plants to low levels of UV radiation from a GE 275-W sunlamp (CG 401-E16RS) to prevent the formation of intumescences on the leaves.

The vines were supported by horizontal bamboo rods extending outward from the pots. New growth was secured weekly with plastic coated wire ties, allowing minimal disruption of the canopy when positioning the plant for labeling and placement of coincidence detectors. The precise geometry of the plant (node

number from the base and length, petiole length and position, and leaf blade length and width) was ascertained several days before each run. This determination allowed precise positioning of detectors and knowledge of their exact location from the source leaf.

Individual plants with mainstems 55 to 60 cm in length, numerous lateral branches, and having 140 to 160 leaves were placed in their final position with detectors in place at least 24 hr before labeling with $^{11}CO_2$. Previous work (20) with the sweet potato had shown that even slight agitation of the plant prior to labeling would decrease dramatically the transport of photosynthate from the leaves. This decrease also has been observed in other species (9).

Isotope production and on-line chemistry. A continuous flow of ^{11}C was produced by bombarding a stream of $^{12}CO_2$ in a specially constructed target chamber with a ^3He beam (6) (Fig. 1A). A Haver window (0.08-mm thickness) was used and the target chamber cooled with dry ice. The nuclear reaction (3) was ^{12}C (^3He, ^4He)^{11}C with the ^3He beam produced using a 4-MeV Van de Graaff accelerator. This provided a continuous stream of $^{12}CO_2$, $^{11}CO_2$, ^{11}CO, and ^{12}CO, which flowed through a Teflon capillary line from the accelerator to the Phytotron where the labeling experiments were conducted.

To increase and control the specific activity of the CO_2 it was essential to remove the $^{12}CO_2$ and $^{11}CO_2$ present in the stream of gases. This removal was accomplished by passing the gases through an Ascarite column, which removed CO_2 but not CO. The CO_2 free air then was passed through a heated column of CuO (600°C), which oxidized the ^{11}CO and ^{12}CO to $^{11}CO_2$ and $^{12}CO_2$ (Fig. 1B), resulting in an ≈1000-fold increase in specific activity over the original gas mixture from the target chamber. The gases then were passed through a dew point analyzer to determine the moisture content, an infrared CO_2 analyzer to determine total CO_2 concentration, and a cuvette equipped with a γ-ray detector to determine the specific activity of the gas mixture (Fig. 1C). The flow rate and CO_2 concentration were adjusted with CO_2-free air or air with supplemental CO_2 (21).

Application of $^{11}CO_2$ to the plant. The air containing $^{11}CO_2$ and appropriate CO_2 concentration (375 $cm^3 \cdot m^{-3}$) (tested by bypassing the leaf chamber to the infrared CO_2 analyzer), before passing through a cuvette-detector arrangement to monitor the specific activity of the gas (''In Monitor''). The air with $^{11}CO_2$ then moved into a specially constructed clear plastic Lexan leaf chamber with a water jacket on the top and bottom of the leaf (Figs. 1D and 2). The chamber was constructed of a 2-mm-thick closed-pore neoprene gasket on each water jacket. The gas was passed over the upper surface of the leaf (20 cm^2), exited the opposite end, then entered the lower chamber, passing over the lower surface of the leaf. The exiting gas then moved through a second cuvette-detector (''Out Monitor''), where the remaining $^{11}CO_2$ was measured. The $\Delta^{11}CO_2$ then could be determined by subtracting the radioactivity of the ''Out Monitor'' from the ''In Monitor'' and correcting for decay and detector sensitivity. The gas subsequently flowed through a second infrared CO_2 analyzer and dew point analyzer before passing on to a delay line and vent (Fig. 1C).

Positioned below the leaf chamber was a single γ-ray detector to monitor the build-up of activity within the labeled leaf (Fig. 2). The ''Line'', ''In Monitor'', ''Out Monitor'', and ''Leaf'' detectors were lead-shielded to prevent excitation by other sources of radiation.

Additional detectors were positioned on the plant's main stem at various intervals from the treated leaf to monitor the movement of labeled photosynthates throughout the plant (Fig. 1D). These detectors were positioned as pairs on each side of the main stem to allow coincidence counting (Fig. 3). Because the energy level of the emitted γ-rays was sufficiently high to excite any unshielded detectors in the room, interference by peripheral radiation was eliminated by time-coincidence counting. Since two γ-rays are emitted from a single positron at an 180° orientation from one another, the paired detectors were electronically required to ''see'' both γ-rays simultaneously, thus allowing precise localization of the source (decaying ^{11}C) and minimization of undesired background. The geometry of the paired detectors and the stem was therefore critical. This geometry was standardized using specially constructed plastic foam fittings (Fig. 2). Generally, five pairs of detectors in addition to the single detectors previously mentioned were used; one on the petiole of the treated leaf, one on the main stem above the treated leaf, and three on the main stem below the treated leaf (Fig. 1D). One additional shielded detector was placed on the medium surface over the developing storage roots.

The detectors consisted of either NE 102 (singles detectors) or CsF (coincidence detectors) optically coupled to photomultiplier tubes. Each detector or set of paired detectors were calibrated prior to and after each run using a specially configured γ-ray source (^{22}Na).

Signal processing and counting. Signals from the detectors were processed using a standard nuclear instrumentation electronics modular (NIM) and counted with a computer-automated measurement and control system (CAMAC) (Fig. 1E). Modules in the CAMAC also received signals from the CO_2 infrared analyzers, dew point analyzers, and flow meters. The CAMAC was interfaced with a Hewlett Packer 9845B (option 250) microcomputer with 186Kbyte memory. This system allowed CRT graphic display of the experimental data in real time as the experiment progressed and direct screen copies using a thermal printer. Raw data inputs were displayed every 60 sec on the CRT during the course of the experiment. The specialized software for data handling and manipulation was developed by one of us (C.E.M.). Additional details on signal processing and counting have been published previously (21).

Data manipulation and parameters measured. Due to the high energy of emitted γ-rays and the short half-life of ^{11}C (20.4 min), a number of computations must be made during the processing of raw data. These computations include corrections for background (background counts for coincidence counters were typically 10 to 12 counts/min), induced background, calibration sensitivity of each detector or pair of detectors, geometry of the detectors, relative specific activity ($^{11}CO_2/^{12}CO_2$), and decay of ^{11}C during transit. In addition, data inputs were made for plant geometry, detector location on the plant, leaf chamber area, and flow rate, which were used in several specific computations. All raw data were processed using a smoothing routine to minimize random data spikes (24).

We measured the characteristics of the carbon acquisition, transport, and allocation system within the sweet potato listed in Table 1.

In order to obtain both time-dependent and steady-state information, we used an extended square wave of radioactivity, which gave a leading edge, a steady-state portion, and a tailing edge once labeling was discontinued. Carbon allocation within the leaf was treated as a two-compartment system, where activity from the storage compartment is lost only by isotope decay and activity in the export department is lost both by decay and

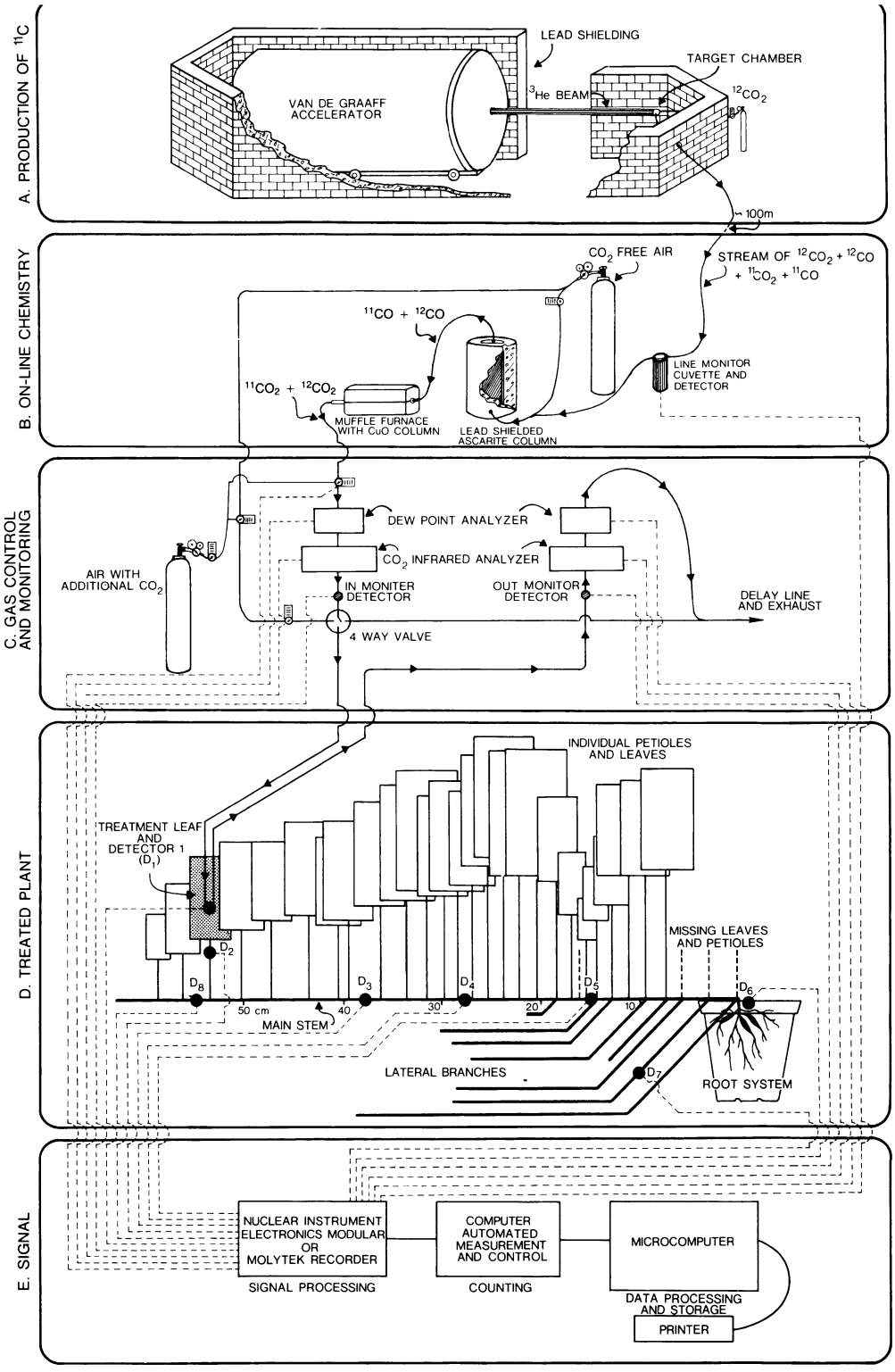

Fig. 1. Schematic presentation of the system used for the steady-state production of ^{11}C and measurement of its introduction into and transport within a sweet potato plant. (**A**) ^{11}C is produced by bombarding a flowing stream of $^{12}CO_2$ in a specially constructed target chamber with a beam of ^{3}He from a Van de Graaff accelerator (4 MeV) (**B**) The carbon products of the reaction ($^{11}CO_2$, ^{11}CO, $^{12}CO_2$, and ^{12}CO) are transported to an on-line chemistry station within the Phytotron. Carbon dioxide is removed from the air stream using a shielded ascarite column. The remaining carbon monoxide (^{11}CO and ^{12}CO) is oxidized by passing the gas through a CuO column at 600°C. (**C**) The air containing $^{11}CO_2$ is monitored for flow rate, moisture, CO_2 concentration, and specific activity (''In Monitor''). Air with additional CO_2 or without CO_2 is added to maintain the CO_2 concentration at 375 $cm^3 \cdot m^{-3}$. Labeled and unlabeled mixtures arrive at a 4-way valve where one of the streams is selected to flow to the leaf while the other is diverted through the exhaust system. (**D**) The air containing $^{11}CO_2$ enters a leaf chamber (see Fig. 2), passing over the upper surface of the leaf then over the lower surface. It then moves to an ''Out Monitor'' (**C**) to determine the change in radioactivity, and a CO_2 analyzer and dew point meter before passing into a delay line and vent. The plants (**D**) had detectors (denoted as D_{1-8}) at various positions on, above, and below the treated leaf. Illustrated is the precise position of each leaf and lateral branch from the base of a representative plant and the length of the individual petioles and leaf blades. (**E**) Electrical signals from the various detectors and other monitoring equipment were fed into a nuclear instrument electronic module for signal processing, then to a computer-automated measurement and control unit for quantification and finally to a HP microcomputer for data processing and storage.

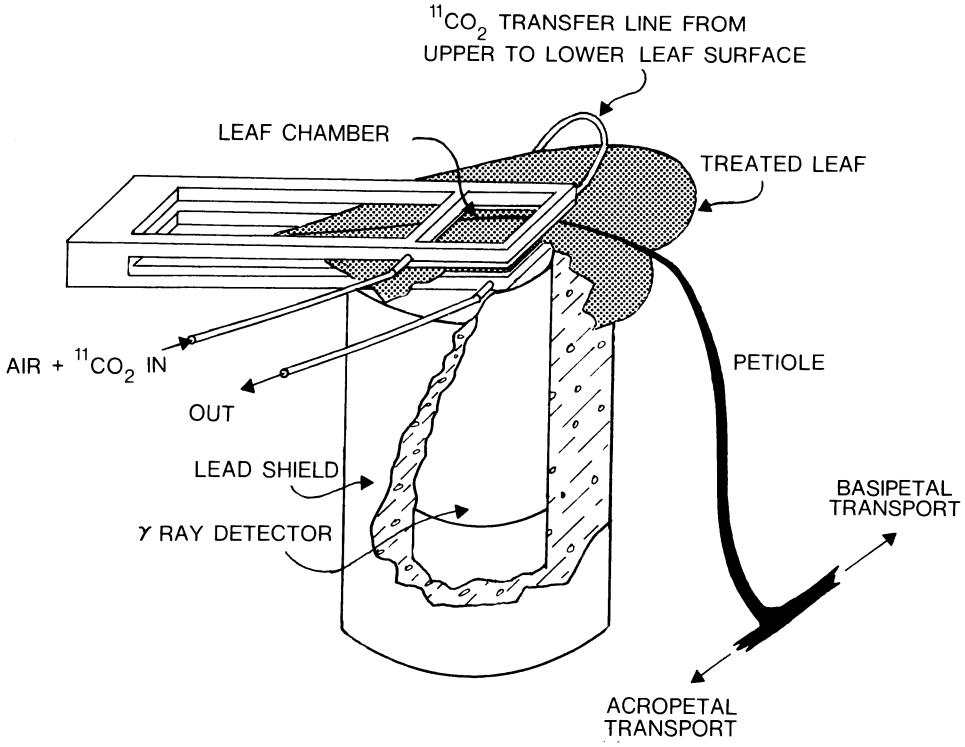

Fig. 2. Air containing $^{11}CO_2$ was introduced into a water-jacketed leaf chamber constructed of clear Lexan plastic. The leaf chamber portion was constructed with a 2-mm-thick, closed-pore neoprene gasket on each water jacket. The ^{11}C-containing air passed over the top of the leaf, exited through a transfer line, then passed over the bottom of the leaf. The exhaust air was then monitored as described in Fig. 1C. Directly beneath the treated area of the leaf was a single lead shielded γ-ray detector. Located on the petiole 2 cm below the base of the leaf blade (not shown) was a pair of coincidence γ-ray detectors (i.e., see Fig. 3) for monitoring the exit of label from the leaf blade.

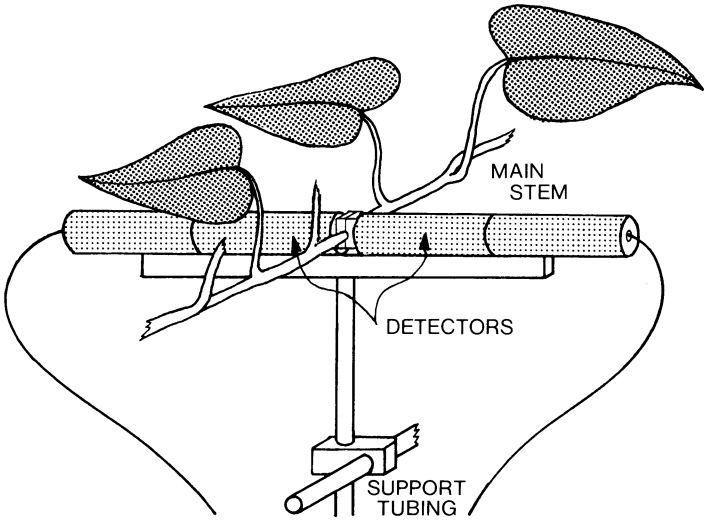

Fig. 3. A pair of detectors for coincidence counting were positioned at various places on the plant. Special mounting apparatus for the detectors and holding blocks for the stem allowed precise positioning of the detectors.

Table 1. Characteristics of the sweet potato carbon acquisition, transport, and allocation system.

Parameter	Unit of measurement
Leaf	
Net rate of ^{11}C assimilation	nCi·cm $^{-2}$·s $^{-1}$
Rate of export of ^{11}C photosynthate from the leaf	nCi·cm $^{-2}$·s $^{-1}$
Rate of storage of ^{11}C photosynthate in the leaf	nCi·cm $^{-2}$·s $^{-1}$
Turnover time of the export pool	minutes
Percent export	%
Steady-state ^{11}C activity of the export pool[z]	nCi·cm $^{-2}$
Transport	
Speed of photosynthetic transport throughout the plant	cm·min $^{-1}$
Mean transit time to various sites in the plant	minutes
Average steady-state activity at the various sites	nCi/cm (stem) per cm^2 (treated leaf area)

[z]Proportioned to the concentration of the export pool.

export (i.e., replaced by ^{12}C in a steady-state turnover of carbon). There may be small respiratory losses from both pools during the washout period, however. These are not of sufficient size to be resolved by the tracer kinetic analysis. Parameters such as carbon exchange rates, relative pool sizes, turnover rate, and export rate were calculated through the analysis of the leaf radioactivity loss curve after cessation of steady-state labeling. For a detailed description of the theoretical assumptions and mathematics used to analyze steady-state and time dependent curves of the isotope within the leaf, see Fares et al. (7).

The net storage rate was determined from the amount of ^{11}C remaining in the leaf after cessation of labeling (corrected for half-life, background, and induced background) (Fig. 4). The export component was calculated from the slope of the washout curve, which we and others have found to follow a simple exponential function (7). The total rate of assimilation was the composite of the storage rate and the export rate. Export turn-

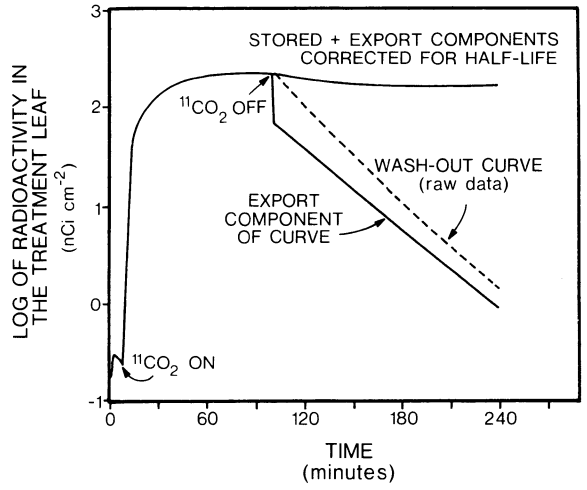

Fig. 4. Typical plot for the loss of radioactivity from the labeled leaf following the cessation of steady state labeling. After cessation of labeling, three curves are obtained: a "wash out" curve of the uncorrected raw data; the loss of activity after correction for the half-life of the isotope, which represents the composite of both the storage and export components; and the export component of the curve (i.e., storage component subtracted out).

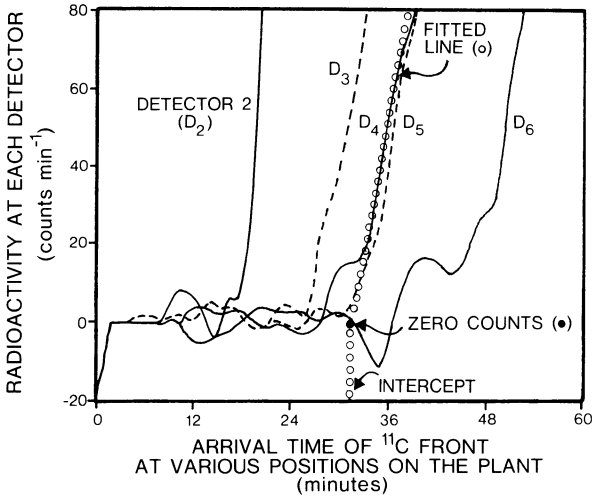

Fig. 5. The arrival time of the ^{11}C-labeled photosynthate front at each set of detectors (D_2–D_6) was determined using an expanded arithmetic plot of the counts/min at each detector (corrected for background and induced background). For each upward trace a line was fitted (circles) from the first data point above 10 CPM through the next 15 points upward (60-sec intervals). The time where the fitted line extrapolated to zero CPM was the arrival time of the ^{11}C-labeled photosynthate at that detector.

over time was determined from the steady-state activity level in the export pool and the rate of export of label from the export pool.

Transport speeds between various positions on the plant were calculated from the arrival time of the ^{11}C front at each pair of detectors minus the arrival time at the nearest upstream detectors and the distance (centimeters) between the respective pairs of detectors on the stem. Arrival time was determined by using an expanded arithmetic plot (Fig. 5) of the counts/min in paired detectors along the transport path (corrected for background, induced background). Arrival of the ^{11}C front at each position was indicated when counts in the coincidence detectors increased sharply (Fig. 5) (i.e., >1% of the final level). A line was then fitted from the first data point above 10 CPM through the next 15 points upward (60-sec intervals). The time where this fitted line extrapolated through zero CPM was used as the arrival time. Distances between individual detectors were calculated automatically from X–Y coordinates entered at the beginning of the experiment and the mean transit speed (cm·min^{-1}) determined between each set of coincidence detectors.

Experimental protocol. To determine changes in the carbon fixation, transport, and allocation system of the sweet potato during the day, we exposed plants three times during the normal 15-hr light period to a 1.5-hr square wave of $^{11}CO_2$. This labeling pattern allowed all points on the plant to approach steady-state. At that time, the treated leaf was switched from $^{11}CO_2$ to $^{12}CO_2$. The loss of label throughout the plant was monitored over the next 2.5 hr. At the end of this time interval, the radioactivity in the plant approached background levels.

Simultaneous runs were made on two uniform plants at a time. Additional runs were made during the course of these experiments and over the previous 2.5 years. Since each test plant was unique, it was not possible to use exactly the same geometry for the detectors. As a consequence, it was not possible to calculate a meaningful average for specific parameters over several plants. However, the results were identical in trend and general magnitude for other plants similarly treated in this series of experiments.

The carbon fixation, translocation, and allocation system in the sweet potato was measured during the morning (beginning ≈2.5 hr after the lights came on), mid-day (beginning at the 7th hr), and in the late afternoon (beginning at the 13th hr or 2 hr before dark) of a 15-hr photoperiod. Because of the short half-life of ^{11}C, the experiment could be conducted at each time period on the same plants.

Test plants had main stems ≈60 cm in length with 28 to 30 fully expanded leaves. Lateral branches (7 to 8 per plant), ranging from 3 to 43 cm in length with 3 to 16 open leaves, had developed from the lower nodes (e.g., nodes 1, 2, 4, 5, 7, 8, and 12). In addition, the plants possessed young storage roots (6 to 8) generally 8 to 12 cm long and 0.6 to 1.4 cm in diameter. The total leaf area of the plants at this stage in their growth was ≈4000 to 4500 cm^2.

The leaf selected for the introduction of $^{11}CO_2$ was the most recent fully expanded leaf toward the apex of each plant (node 28 of plant illustrated in Fig. 1D). Generally there were four to six opened but not yet fully expanded leaves above this position.

The first pair of coincidence detectors was placed on the petiole of the treated leaf 2 cm below the base of the leaf blade. The second pair of detectors was positioned below the treated leaf on the main stem between nodes 26 and 27. Subsequent pairs were positioned between nodes 22 and 23, 17 and 18, and 8 and 9 (Fig. 1D). One pair of detectors was placed on a lateral branch that had developed from the second node, 20 cm outward from the main stem. One additional set of coincidence detectors placed on the internode immediately above the petiole of the treatment leaf. This placement allowed monitoring acropetal transport of photosynthate. A single lead shielded detector was placed at the base of the plant on the media surface to monitor the movement of ^{11}C-labeled photosynthate into the general area of the storage roots.

Parameters that were identical at each run during the day were: gas volume of the $^{11}CO_2$ leaf chamber = 7 cm^3; leaf area treated = 20 cm^2; input and output flow of gas through the leaf chamber = 7.3 cm^3·s^{-1}; specific activity = 0.210 Ci·mol^{-1}; leaf temperature = 27.3°C; and dew point of the gas

entering the chamber = 17.5°. Parameters that varied during the morning (AM), mid-day (MD), and afternoon (PM) treatment periods were: maximum phloem counts = 5200 (AM), 5000 (MD), and 3400 (PM) CPM; transpiration = 179 (AM), 168 (MD), and 124 (PM) nM H_2O/cm^2 per sec [standard deviations for mean transpiration rates of test leaves were ± 21 (AM), ± 18 (MD), ± 16 (PM); for CER ± 0.21 (AM), ± 0.17 (MD), ± 0.22 (PM); and for stomatal resistance, ± 0.13 (AM), ± 0.18 (MD), ± 0.04 (PM).]; dew point of the gas exiting the leaf chamber = 25.6° (AM), 25.2° (MD), and 23.5° (PM); mean CO_2 concentration of the gas entering the leaf chamber = 375 (AM), 370 (MD), and 375 (PM) $cm^3 \cdot m^{-3}$; carbon exchange rate 1.15 (AM), 1.21 (MD), and 1.04 (PM) $nM \cdot cm^{-2} \cdot s^{-1}$, stomate resistance = 0.590 (AM), 0.860 (MD) and 2.18 (PM) $cm^2 \cdot s^{-1}$ and the ΔCO_2 in the leaf chamber = 70.7 (AM), 74.1 (MD), and 64.0 (PM) $cm^3 \cdot m^{-3}$. These changes represent the normal cyclic pattern of photosynthesis in the sweet potato during the day.

Results and Discussion

Changes in leaf photosynthate during the day. The size of the export pool of photosynthates within the treated leaf varied substantially with time of day (Fig. 6A). The export pool was largest during the morning (AM) and late afternoon (PM) when a substantially greater proportion of the fixed carbon was being translocated out of the leaf. During mid-day, the export pool size was nearly 32% lower than the late afternoon. Likewise, the rate of export of photosynthates from the treated leaf changed during the day (Fig. 6B). Highest export rates (i.e., 0.715 $nM \cdot cm^{-2}s^{-1}$) were found in the morning, declining at mid-day, and increasing only slightly toward the late afternoon. Therefore, while the size of the export pool increased late in the day, there was not a commensurate rise in the rate of export. In contrast to the rate of export, the storage rate of photosynthate within the treated leaf increased during mid-day (Fig. 6C), indicating that the treated leaf favored the export of photosynthate during the early portion of the day. Toward mid-day, this shifts in favor of the temporary storage of photosynthate in the leaf. Storage declines late in the day, without a commensurate rise in export. Thus, there is a sharp increase in the size of the export pool.

This change in the carbon allocation pattern during the day can also be seen in the shift in the relative ratio (expressed as percent) of the photosynthate that is stored in the leaf vs. that translocated out of the leaf (Fig. 7 top). The percent export is greatest during the morning (AM) and late afternoon (PM), with peak storage periods around mid-day. There is a progressive rise in the turnover time of the export pool from early morning (19 min) until late afternoon (27 min) (Fig. 7 bottom), indicating a slower absolute flux of photosynthate through the pool. This rise can be altered by both pool size and export rate. The longest turnover time (PM) coincides with the greatest pool size (1364 $nM \cdot cm^{-2}$) (Fig. 6A). At mid-day, the export pool size was at its minimum; however, the rate of export was also at its minimum. Therefore, the effect of the smaller export pool size on the turnover time of the export pool was in part compensated for by changes in the rate of export during the peak periods of photosynthate storage at mid-day.

The build-up of starch in the leaves during the light period is a well-known phenomenon (1, 2, 8, 22, 25). This starch appears to be hydrolized and recycled out of the leaf largely during the dark period. Several factors are known to modulate the flow of photosynthetic carbon between the storage and transport pools.

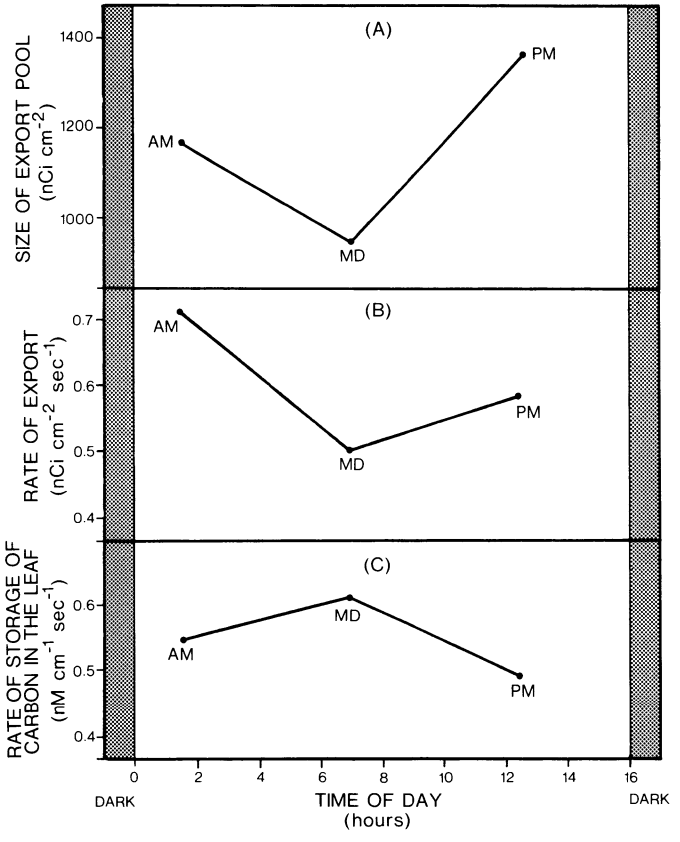

Fig. 6. Changes in (**A**) the size of the export pool of photosynthate within the labeled leaf; (**B**) the rate of export of photosynthate from the treated leaf; and (**C**) the storage rate of photosynthate within the treated leaf at three times during the day [AM, mid-day (MD), and PM].

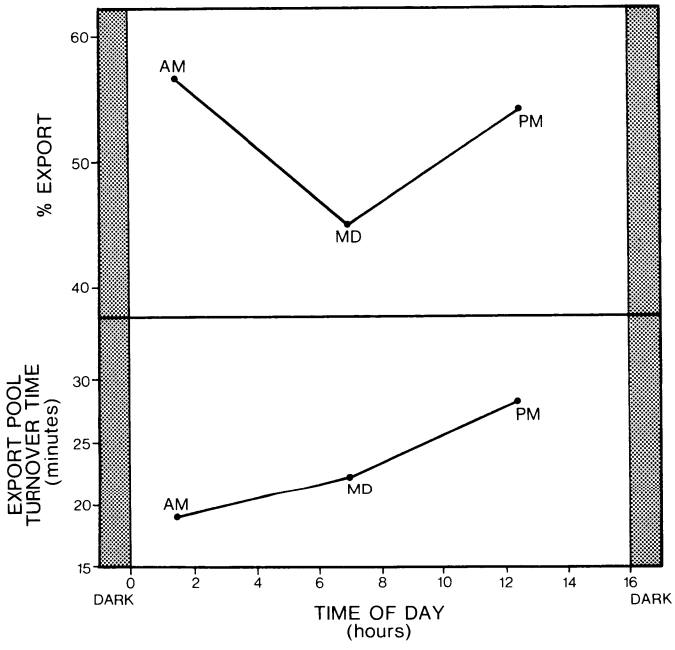

Fig. 7. Changes in the percentage of fixed carbon exported from the treated leaf (**upper**) and the turn-over time of the export pool of photosynthate within the treated leaf at three times during the day [AM, mid-day (MD), and PM] (**lower**).

For example, the ratio of starch to sucrose is controlled a) genetically (13); b) by sink demand (22, 23), and c) by the rate of carbon assimilation (5).

Apical leaves in the sweet potato undergo a significant shift in the allocation of newly fixed carbon as the light period progresses. Early in the day, transport of carbon from the apical leaves predominated over storage as starch. During this time, the percent export of carbon reached ≈57% (Fig. 6A). By midday, the percent export had declined by nearly 12%, with the storage of carbon within the leaf now favored. Late in the day, the percent export again increased. This increase could be caused by a decreased demand for starch synthesis in the chloroplasts, increased sink demand for photosynthates, a decreased rate of carbon assimilation, or other mechanisms.

Accompanying these shifts in the flow of carbon between leaf storage and export pools are changes in other leaf parameters. There were significant changes in the size of the export pool of carbon within the leaf and in the turnover time of the export pool. These alterations do not precisely mirror changes in the allocation of carbon between storage and export functions, however. For example, increases in the turnover time of the export pool during the day are not closely correlated with changes in the size of the export pool, indicating that factors in addition to pool size modulate the rate of movement of carbon through the pool.

Translocation of photosynthate. The transport speed of photosynthate from the treated leaf was not uniform throughout the plant (Fig. 8). The speed in the morning (AM) was relatively low (i.e., 1.4 cm·min^{-1}) between the petiole of the treated leaf [detector 2 (D_2)] and the first detector below the treated leaf (D_3). This speed also was found for the transport of the photosynthate between the most basipetal detector on the main stem (D_5) and the root system (D_6). Between detectors 3 → 4 and 4 → 5, the speed of the photosynthate within the phloem increased dramatically during the early morning.

At mid-day, the transport speed remained relatively constant between the uppermost detectors below the treatment leaf and the basipetal detector positions (i.e., $D_2 \rightarrow D_3$ and $D_5 \rightarrow D_6$). Mid-day transport velocities between $D_3 \rightarrow D_4 \rightarrow D_5$ remained significantly higher than both more apical and basepetal segments of the main stem, but had declined considerably from the morning rates.

By late afternoon, the mid-stem detectors ($D_3 \rightarrow D_4 \rightarrow D_5$) had declined to their lowest speeds measured during the day, while the velocity of the initial petiole-stem segment ($D_2 \rightarrow D_3$) had increased substantially. This increase in speed of photosynthate from the leaf late in the day was consistent for all plants tested. Likewise, the velocity of photosynthate between detectors $D_4 \rightarrow D_5$ was consistently higher at this time of day than for the segment of the main stem immediately above it.

Differences in transport speeds along the stem have been noted previously for *Ipomoea nil* Roth. (4). Variations in speed noted in their experiments were inconsistent and did not form a distinct pattern along the stem (e.g., increasing or decreasing progressively toward the base of the plant). The lack of consistency in the differences in speeds may have been due to both the relatively low transport speeds of the species (i.e., 0.6 to 1.0 cm·min^{-1}) and the substantial distance between detectors. Large distances would result in an integration of slower and faster rates along the stem (described later).

Differences in transport velocities between various sites along the main stem may perhaps be due to influxes of photosynthate from other leaves along the stem and/or changes in the resistance to flow once the photosynthate enters the phloem traces of the main stem. The low transport speeds between the petiole (D_2) and the first basipetal detector (D_3) on the main stem in this study would indicate restricted movement within the petiole and/or from the petiole into the main stem.

While changes in the transport speed of photosynthate within specific segments of the main stem is of considerable interest,

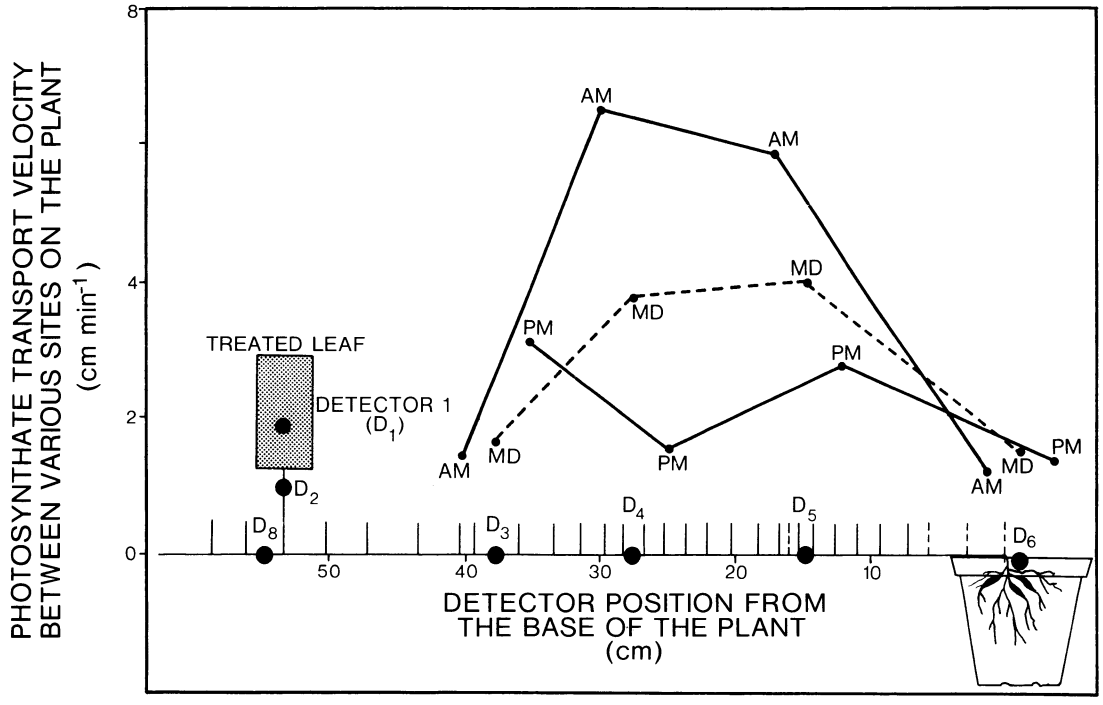

Fig. 8. Mean photosynthate transport velocity between various basipetal positions on the main stem at three times during the day [AM, midday (MD), and PM].

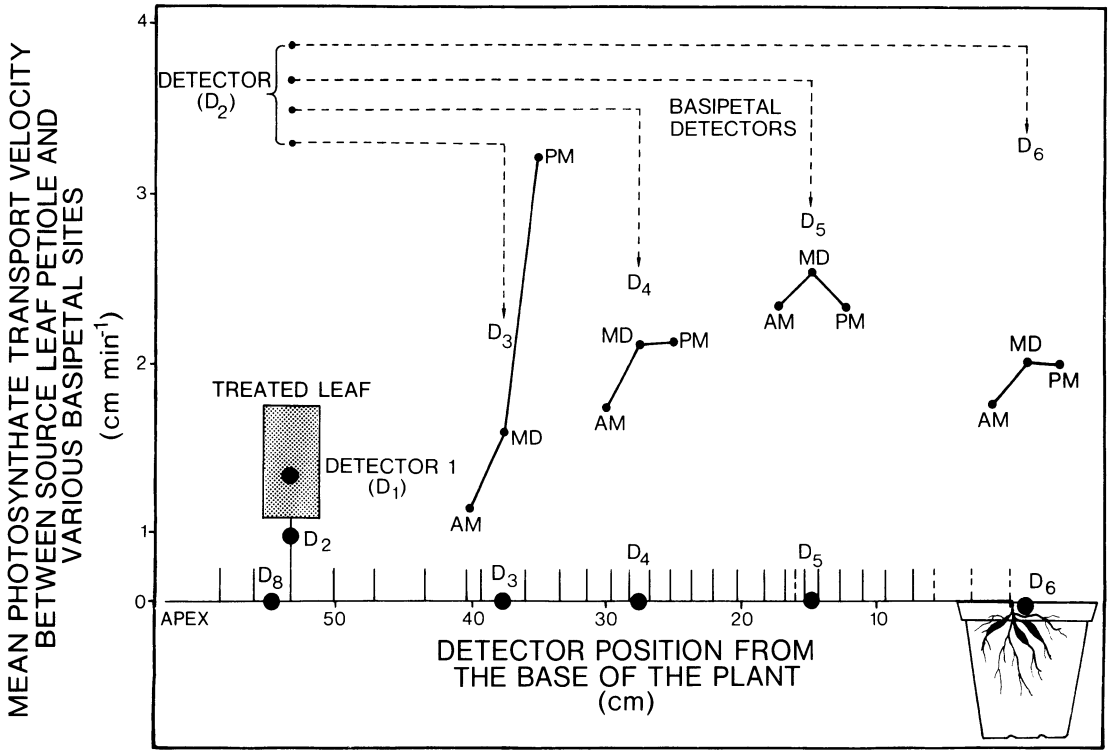

Fig. 9. Changes in the mean transport velocity of photosynthates between the petiole of the treated leaf (detector 2) and various basipetal positions on the mainstem from the treated leaf at three times during the day [AM, mid-day (MD), and PM].

the net effect on arrival time at specific sites (e.g., storage roots) is critical. Illustrated in Fig. 9 are the mean transport speeds of photosynthate from the top of the petiole of the treated leaf (D_2) to various basipetal positions on the main stem.

Generally, the mean speed from the petiole of the treated leaf to various sites below ranged from 1.8 to 2.5 cm·min^{-1}. There was typically an increase in speed toward the base of the main stem and a decline in velocity as the photosynthate entered the root zone. The latter may be partially artificial, since only a single detector was used over the root system and it surveyed a much broader area. Highest transport rates were found in the late afternoon (PM) for movement out of the petiole to the initial detector on the main stem below the treated leaf. Thus, while the mean speed of photosynthate between the treated leaf to various points down the main stem appears relatively uniform, mean speed represented the composite effect of differential speeds along the transport path. Thus, the greater the distances between detectors [in the case of Christy and Fisher (4) the detectors were ≈30, 110, and 230 cm below the treated leaf], the greater the degree of integration of the varying transport speeds.

The mean velocities for 'Jewel' (≈2.0–2.5 cm·min^{-1}) were comparable to those reported for 'Okinawa No. 100' (2.13 cm·min^{-1}) (17). Both cultivars displayed considerably higher transport speeds than 'Centennial' (20). Thus, there exists a considerable range in the rate at which photosynthates are transported both within the genus *Ipomoea*, between cultivars of the species *I. batatas*, and within individual plants.

To determine the relative amount of acropetal to basipetal transport, we calculated the average ^{12}C equivalents of photosynthate at each detector (Fig. 10). It is evident from the acropetal detector (D_8) placed on the internode immediately above the petiole of the treated leaf that virtually no carbon is translocated from the treated leaf toward the growing shoot tip during the day. Growth of the main stem apex appears then to be dependent upon either carbon recycled from the storage pool within the apical leaves during the night or that provided by more apical (or, less likely, more basal) leaves on the plant.

These results differ distinctly from those described for 'Okinawa 100' (18). Here, both apical and basal leaves exhibit bidirectional transport, with the lower leaves transporting a greater percentage of their fixed carbon in a basipetal direction. The two cultivars represent selections from distinctly different gene pools. The results, as a consequence, suggest that there is a significant range in the carbon allocation pattern within the species.

While acropetal transport was negligible, a significant amount of photosynthate was translocated into a basal lateral branch. Hence, lateral branches exhibited acropetal transport of carbon derived from apical leaves on the main stem. The lateral branches tested typically had a number of fully expanded leaves capable of photosynthate export. From the arrival time of the photosynthate at the coincidence detectors on the lateral branches, it is not entirely clear if the photosynthate moves directly into the lateral branch or first moves to the root system and then is transported into the lateral.

Differences in the average ^{12}C equivalents of photosynthate during the day reflect the increased storage of carbon within the leaf during mid-day (Fig. 10). Highest concentrations occurred early in the morning at all sites.

The greatest concentration of photosynthate exterior to the treatment leaf was in the root system (Fig. 10). The plants had, at this time, developing storage roots that represent the major site for carbon deposition within the plant. By the end of the growing season, the storage roots comprise ≈65% of the total plant dry matter with the fibrous roots representing only 0.8% (26). Differences in photosynthate at the three pairs of detectors

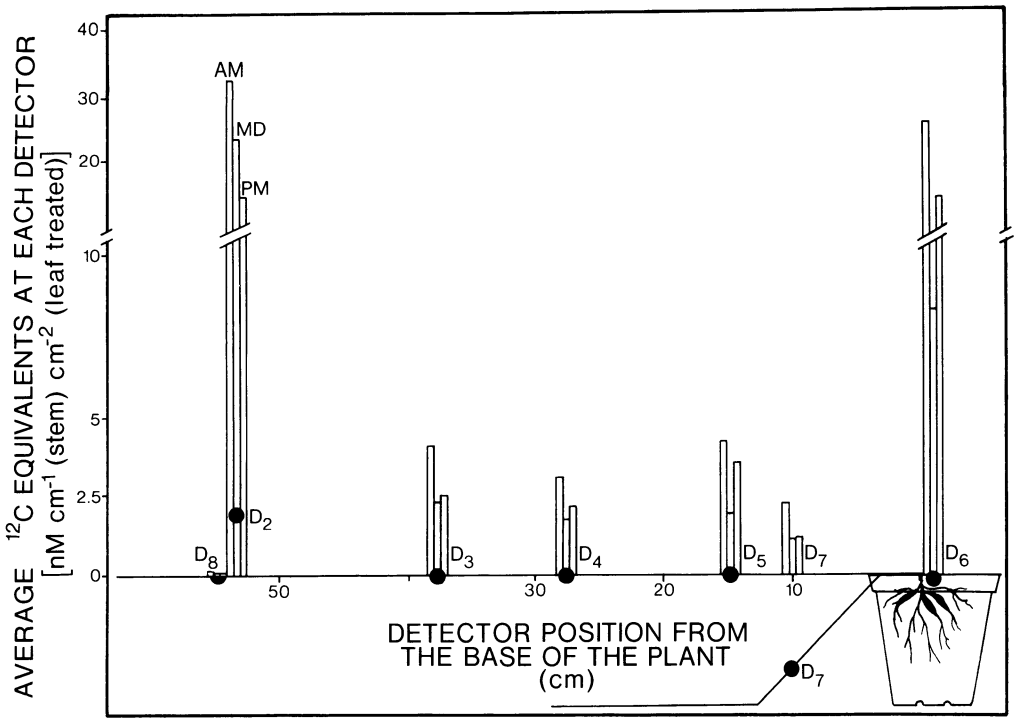

Fig. 10. The average ^{12}C equivalents of photosynthate from the treated leaf at each detector and changes in the concentration at three times during the day [AM, mid-day (MD), and PM].

along the main stem (D_{3-5}) may represent small differences in phloem unloading along the transport site. Occasionally detectors that include a small developing axillary bud within their window displayed higher accumulations.

Literature Cited

1. Chang, W.C. 1980. Starch depletion and sugars in developing cotton leaves. Plant Physiol. 65:844–847.
2. Chatterton, N.J. and J.E. Silvius. 1979. Photosynthate partitioning into starch in soybean leaves. Plant Physiol. 64:749–753.
3. Cirilov, S.D., J.D. Newton, and J.P. Schapira. 1966. Total cross sections for the reaction $^{12}C(^3He, ^4He)^{11}C$ and $^{12}C(^3He, \eta)^{14}O$. Nuclear Phys. 77:472–476.
4. Christy, A.L. and D.B. Fisher. 1978. Kinetics of ^{14}C-photosynthate translocation in morning glory vines. Plant Physiol. 61:283–290.
5. Fader, G.M. and H.R. Koller. 1983. Relationships between carbon assimilation, partitioning and export in leaves of two soybean cultivars. Plant Physiol. 73:297–303.
6. Fares, Y., D.W. DeMichele, J.D. Goeschl, and D.A. Baltuskonis. 1978. Continuously produced high specific activity ^{11}C for studies of photosynthesis, transport and metabolism. Intl. J. Applied Radiat. Isotopes 29:431–441.
7. Fares, Y., C.E. Magnuson, J.D. Goeschl, and B.R. Strain. 1985. Analysis of carbon allocation in leaves using extended square wave input of continuously produced $^{11}CO_2$. Phytokinetics. Tech Rpt. 1. College Station, Texas.
8. Fondy, B.R. and D.R. Geiger. 1985. Duirnal changes in carbon allocation: morning, p. 358–361. In: R.L. Heath and J. Preiss (eds.). Regulation of carbon partitioning in photosynthetic tissue. Proc. 8th Annu. Symp. Plant Physiol., Amer. Soc. Plant Physiol., Rockville, Md.
9. Goeschl, J.D., C.E. Magnuson, Y. Fares, C.H. Jaeger, C.E. Nelson, and B.R. Strain. 1984. Spontaneous and induced blocking and unblocking of phloem transport. Plant, Cell & Env. 7:607–613.
10. Hahn, S.D. 1977. A quantitative approach to source potentials and sink capacities among reciprocal grafts of sweet potato varieties. Crop Sci. 17:559–562.
11. Hozyo, Y. and C.Y. Park. 1971. Plant production in grafted plants between wild type and improved variety of *Ipomoea*. Bul. Nat. Inst. Agr. Sci. Serv. D22:145–164.
12. Hozyo, Y., T. Murata, and T. Yoshida. 1971. The development of tuberous roots in grafted sweet potato plants, *Ipomoea batatas* Lam. Bul. Nat. Agr. Sci. Serv. D22:165–189.
13. Huber, S.C., P.S. Kerr, and W. Kalt-Torres. 1985. Regulation of sucrose formation and movement, p. 199–214. In: R.L. Heath and J. Preiss (eds.). Regulation of carbon partitioning in photosynthetic tissue. Proc. 8th Annu. Symp. Plant Physiol., Amer. Soc. Plant Physiol., Rockville, Md.
14. Kato, S. and Y. Hozyo. 1972. Translocation of ^{14}C-photosynthates in grafts between the wild type and improved variety in *Ipomoea*. Proc. Crop Sci. Soc. Jpn. 41:496–501.
15. Kato, S. and Y. Kozyo. 1974. Translocation of ^{14}C-photosynthates in several growth stages of the grafts between improved variety and wild type plants in *Ipomoea*. Bul. Nat. Inst. Agr. Sci. Serv. D25:31–58.
16. Kato, S. and Y. Hozyo. 1976. The interrelationship between translocation of ^{14}C-photosynthate and $^{14}CO_2$ exposed leaf position on the grafts of *Ipomoea*. Proc. Crop Sci. Soc. Jpn. 45:351–356.
17. Kato, S. and Y. Hozyo. 1978. The speed and coefficient of ^{14}C-photosynthates translocation in the stem of grafts between improved variety and wild type in *Ipomoea*. Bul. Nat. Inst. Agr. Sci. Ser. D29:113–131.
18. Kato, S., Y. Hozyo, and K. Shimotsuko. 1979. Translocation of ^{14}C-photosynthate from the leaves at different stages of development in *Ipomoea* grafts. Jpn. J. Crop. Sci. 48:254–259.
19. Kays, S.J. 1985. The physiology of yield in the sweet potato, p. 79–132. In: J. Bouwkamp (ed.). Sweet potato products: A natural resource for the tropics. CRC Press, Boca Raton, Fla.
20. Kays, S.J., L.K. Chua, J.D. Goeschl, C.E. Magnuson, and Y. Fares. 1982. Assimilation patterns of carbon in developing sweet potatoes using ^{11}C and ^{14}C, p. 95–118. In: R.L. Villareal and

T.D. Griggs (eds.). Sweet Potato. Asian Veg. Res. & Dev. Center, Tainan, Taiwan.
21. Magnuson, C.E., Y. Fares, J.D. Goeschl, C.E. Nelson, B.R. Strain, C.H. Jaeger, and E.G. Bilpuch. 1982. An integrated tracer kinetics system for studying carbon uptake and allocation in plants using continuously produced $^{11}CO_2$. Radiat. Env. Biophys. 21:51–65.
22. Pharr, D.M., S.C. Huber, and H.N. Sax. 1985. Leaf carbohydrate status and enzymes of translocate synthesis in fruiting and vegetative plants of *Cucumis sativus* L. Plant Physiol. 77:104–108.
23. Rufty, T.W. and S.C. Huber. 1983. Changes in starch formation and activities of sucrose phosphate synthase and cytoplasmic fructose-1,6-bisphosphate in response to source-sink alternations. Plant Physiol. 72:474–480.
24. Tukey, J.A. 1977. Exploratory data analysis, Addison-Wesley, Reading, Mass.
25. Upmeyer, D.J. and H.R. Koller. 1973. Diurnal trends in net photosynthetic rate and carbohydrate levels of soybean leaves. Plant Physiol. 51:871–875.
26. Yoshida, T., Y. Hozyo, and T. Murata. 1970. Studies on the development of tuberous roots in sweet potato (*Ipomoea batatas*, Lam. var. *edulis*, Mak.). The effect of deep placement of mineral nutrients on the tuber yield of sweet potato. Proc. Crop Sci. Soc. Jpn. 39:105–110.

J. Amer. Soc. Hort. Sci. 112(3):554–560. 1987.

Effect of Surfactants on Foliar Penetration of NAA and NAA-induced Ethylene Evolution in Cowpea

N.K. Lownds, J.M. Leon, and M.J. Bukovac
Department of Horticulture, Michigan State University, East Lansing, MI 48824

Additional index words. *Vigna unguiculata*, Pace, Tween 20, Regulaid, absorption

Abstract. **Effects of the surfactants Pace, Regulaid and Tween 20 were determined on foliar penetration of NAA and on NAA-induced ethylene production by cowpea [*Vigna unguiculata* (L.) Walp. subsp. *unguiculata* cv. Dixielee]. All three surfactants decreased surface tension of NAA solutions, causing a marked increase in wetting and in droplet : leaf interface area. The greatest increase in NAA penetration was obtained with Regulaid followed by Pace and Tween 20. The surfactant effect was most pronounced during the droplet drying phase, but penetration continued to take place from the deposit after drying. The mode of action of surfactants in enhancing NAA penetration is complex. Regulaid-enhanced penetration closely paralleled the increase in interface area, but similar relationships were not found for Pace or Tween 20, particularly at concentrations above the critical micelle concentration. Surfactant-enhanced NAA penetration caused an increase in NAA-induced ethylene production. There was a strong correlation (r = 0.82) between NAA penetration and ethylene production for doses of 0.5 to 2.5 μg/disk. Above 2.5 μg/disk, ethylene production increased at a decreasing rate. The potential for using auxin-induced ethylene production as an index for quantifying auxin penetration is discussed. Chemical names used: 1-naphthaleneacetic acid (NAA), polyoxyethylene polypropoxypropanol dihydroxypropane (Regulaid), polyoxyethylene (20) sorbitan monolaurate (Tween 20), surfactant blend in paraffin base petroleum oil (Pace).**

Cuticular penetration is a prerequisite for the physiological action of foliar-applied systemic compounds (3, 17, 19). Thus, chemicals often are formulated specifically with surfactants to improve the physical : chemical characteristics of the spray solution to enhance wetting (8, 10, 13) and penetration.

The effects of surfactants on penetration have not been well-defined (18, 20). Surfactants that enhance penetration generally increase wetting as concentration is increased up to the critical micelle concentration (CMC). With a further increase in concentration, there is little or no additional enhancement of wetting or penetration. However, with some surfactants, penetration may be increased at concentrations above the CMC (18, 20, 22). This increase would suggest surfactant effects beyond that commonly attributed to improved wetting (2, 8, 17).

The effects of surfactant concentrations above the CMC on growth regulator performance and on plant processes largely have been ignored. Surfactant concentrations in the range of 0.1% to 1.0% are of particular concern in low-volume spray application where, while maintaining a constant pesticide dose, the concentration of constituents in solution is increased in proportion to the decrease in carrier volume (4). Therefore, when applying formulated agrochemicals, all constituents of the formulation are concentrated, including the surfactant, which may approach 1.0% (15).

NAA induces ethylene production in plants (1, 7, 11, 12), and this response may be useful as a means of quantifying NAA penetration (7). Data are not available on the direct relationship between NAA penetration and ethylene production. Further, the effects of surfactants on NAA-induced ethylene production have not been reported. Thus, the objectives of this study were to determine the effects of selected surfactants over a wide range of concentrations on foliar penetration of NAA and to relate these findings to NAA-induced ethylene evolution.

Materials and Methods

Plant material and culture. Cowpea seeds were pregerminated in the dark at 30°C on moist paper towels. Healthy seeds of uniform size and radicle length were selected, seed coats removed to facilitate epicotyl emergence, and planted into disposable AC-4-8 "Cell Paks" (Geo. J. Ball, W. Chicago, Ill.)

Received for publication 31 Oct. 1986. Michigan State Univ. Agricultural Experiment Station Journal Article no. 12148. These studies were supported in part by the USDA under Agreement no. 3607-20300-004-01 S and by a grant from the Shell Development Co., Modesto, Calif. The cost of publishing this paper was defrayed in part by the payment of page charges. Under postal regulations, this paper therefore must be hereby marked *advertisement* solely to indicate this fact.